

Journal Pre-proofs

Preliminary study on terahertz non-destructive testing for defect detection in hot melt joints of polyethylene pipes

Hailiang Nie, Kai Mu, Zhibo Zhang, Yunpeng Ding, Sen Zhao, Ke Wang, Wei Dang, Junjie Ren, Xiaobin Liang, Weifeng Ma

PII: S1350-4495(24)00184-1
DOI: <https://doi.org/10.1016/j.infrared.2024.105300>
Reference: INFPHY 105300

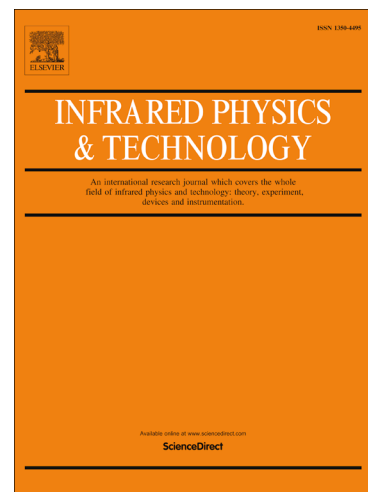
To appear in: *Infrared Physics & Technology*

Received Date: 20 August 2023
Revised Date: 8 January 2024
Accepted Date: 3 April 2024

Please cite this article as: H. Nie, K. Mu, Z. Zhang, Y. Ding, S. Zhao, K. Wang, W. Dang, J. Ren, X. Liang, W. Ma, Preliminary study on terahertz non-destructive testing for defect detection in hot melt joints of polyethylene pipes, *Infrared Physics & Technology* (2024), doi: <https://doi.org/10.1016/j.infrared.2024.105300>

This is a PDF file of an article that has undergone enhancements after acceptance, such as the addition of a cover page and metadata, and formatting for readability, but it is not yet the definitive version of record. This version will undergo additional copyediting, typesetting and review before it is published in its final form, but we are providing this version to give early visibility of the article. Please note that, during the production process, errors may be discovered which could affect the content, and all legal disclaimers that apply to the journal pertain.

© 2024 Published by Elsevier B.V.



Preliminary study on terahertz non-destructive testing for defect detection in hot melt joints of polyethylene pipes

Hailiang Nie^{1*}, Kai Mu², Zhibo Zhang², Yunpeng Ding², Sen Zhao¹, Ke Wang¹, Wei Dang¹, Junjie Ren¹, Xiaobin Liang¹, Weifeng Ma¹

¹*Institute of Safety Assessment and Integrity, State Key Laboratory for Performance and Structure Safety of Petroleum Tubular Goods and Equipment Materials, CNPC Tubular Goods Research Institute, Xi'an, 710077, China*

²*The 7th oil production plant of Changqing Oilfield Branch of petrochina Co., LTD, Gansu, 745000, China*

*Corresponding email: niehailiang@mail.nwpu.edu.cn

Abstract: With the rapid development of the economy and society, non-metallic pipelines are more and more widely used in oil and gas fields, water supply projects, urban gas systems, and so on. Among the conventional nondestructive testing (NDT) methods, only ultrasonic, radiographic, and penetration testing tools are applicable to non-metallic pipe examination from a theoretical perspective, while their actual efficiency is quite low. In this work, terahertz (THz) non-destructive detection of typical welding defects in polyethylene-pipe hot melt joints is carried out. The characteristic THz wave signal is obtained, and the relationship between the THz wave and the defect type is established. Finally, a THz signal processing model for defect detection in polyethylene-pipe hot melt joints is established. Thus, this research lays a foundation for the application of the THz non-destructive testing technology to polyethylene pipeline engineering.

Keywords: Polyethylene pipes; Terahertz waves; Non-destructive testing; Welding defects; Signal modeling

1. Introduction

With the rapid development of the economy and society, the application of non-metallic pipelines to the oil and gas fields is becoming more extensive. The substitution of non-metallic pipes for steel pipes can prevent the external and internal corrosion of the pipe caused by the transportation of highly mineralized sewage and water-containing oil, thus reducing the pipeline maintenance workload. At the same time, it plays an important role in speeding up the pipeline construction and decreasing investment in pipeline construction [1]. In addition, environmental protection, water supply, and urban gas projects are also increasingly using non-metallic pipelines. The safety of non-metallic pipelines has also attracted

increasing attention, and the detection and evaluation of non-metallic pipelines will have great market value and development prospects in the future [2].

Compared with other metal pressure equipment, non-metallic pipes possess no electrical and magnetic conductivity characteristics (except for steel-skeleton plastic-composite pipes). For this reason, among the conventional non-destructive methods, only ultrasonic, X-ray, and penetration testing technologies are feasible for characterizing non-metallic pipes; however, their efficiency is still limited [3-6]. Because of the peculiar features of non-metallic materials to drastically decrease X-ray attenuation, only low exposure energies can be used in X-ray detection to obtain better contrast and improve the defect detection rate [4]. However, a low exposure energy makes the imaging fuzzier, resulting in actual operation difficulties. For ultrasonic detection, the nonlinear ultrasonic-guided wave delay method can be used to localize the structural damage within non-metallic pipelines, but the geometric characteristics of the damage cannot be accurately determined [7]. Additionally, no actual case studies on penetration detection have been reported.

In recent years, the research on structural damage detection of non-metallic pipes has advanced rapidly, mainly focusing on straight pipes and pipe joints of non-metallic pipes [8-11]. Dalhousie University in Canada used piezoelectric ceramics to study the joint damage of non-metallic pipelines [12]. A torsional mode-guided wave probe was designed by École Centrale de Lyon in France to monitor the guided wave response and damage characteristics of non-metallic pipes [13]. The University of Rome in Italy conducted simulations and experimental investigations on groove damage within non-metallic round rods using Gaussian pulse-guided wave excitation [14]. In this work, reasonable theoretical results and satisfactory laboratory data were achieved. However, because of a lack of relevant reports, these methods have not been extended yet from the laboratory to practical engineering applications.

Terahertz (THz) radiation refers to electromagnetic waves with a frequency in the range of 0.1–10 THz (1 THz = 10^{12} Hz), low THz energy level (4.1 meV), good signal-to-noise ratio, and high resolution being used in non-destructive testing [15-17]. At present, THz waves are mainly used in THz communications [18-20], cell detection in biological and medical fields [21-23], environmental molecular detection [24-27], and security systems [28-30]. Concerning the non-destructive testing of non-metallic structures, significant results have been achieved in the layered defect detection within composite materials in the aerospace industry [31-33]. Some scholars have successfully used the THz detection technology to measure the wall thickness of polyethylene pipes, but there are still only few tests on welded joints of polyethylene pipes [34,35]. It has been confirmed that the THz detection technology can detect defects in polyethylene pipe bodies [36], but for pipes, the weld is the weak link. Therefore, the non-destructive testing of weld defects is more meaningful for engineering.

This study aims to use the THz detection technology in the non-destructive testing of non-metallic pipes. The defect modes and causes of polyethylene-pipe welded joints were investigated, and simulation test blocks for the non-destructive detection of typical defects of polyethylene-pipe hot melt joints were developed. THz detection imaging of typical defects of non-metallic pipes was conducted, and a THz detection signal analysis for typical defects of polyethylene-pipe hot melt joints was established for the first time, which lays a foundation for the application of the THz nondestructive testing (NDT) technology to polyethylene pipe engineering.

2. Analysis of welding defects present in hot melt joints

According to their types and characteristic failure modes, the defects emerging in polyethylene hot melt butt joints can be classified as follows.

(1) Incomplete fusion defects

Incomplete fusion defects take their origin from welding factors such as local cracks formed on the fusion surface or weakly entangled local polyethylene molecules, resulting in a sharp decline in joint performance (see Fig. 1).

Incomplete fusion defects indicate that the local molecules of the fused surface are not tightly entangled, which has a serious impact on the life of the joint, giving rise to failure under load. As hot melt butt welding is a type of pressure fusion welding, a certain axial pressure is applied to the pipe in the welding process, causing the appearance of incomplete defects on the fusion surface.

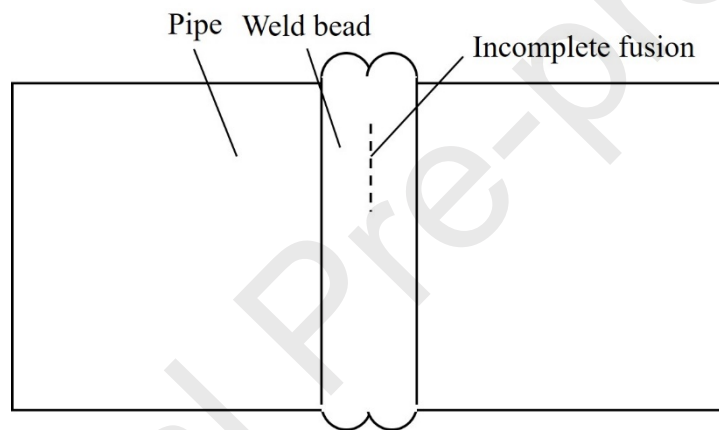


Fig. 1 Schematic of an incomplete fusion defect.

(2) Hole defects

A hole defect is a hole inside the weld generated due to the inclusion of large solid particles or local large shrinkage holes, pores, and other reasons, resulting in a discontinuity of the weld structure and a joint performance reduction. It is a volumetric defect, as shown in Fig. 2.

Hole defects may appear on the fusion surface or in the heat-affected zone near the fusion surface. While the existence of holes deteriorates the mechanical properties of the joint fusion surface, it does not cause the non-fusion expansion failure of the joint like incomplete fusion defects, leading to the ductile fracture of the material near the hole.

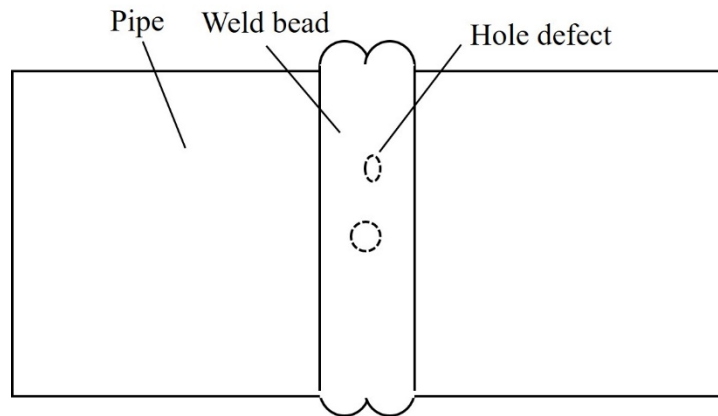


Fig. 2 Schematic of a hole defect.

(3) Inclusion defects

Inclusion defects are due to foreign substances that are mixed in the fusion surface to form heterogeneous inclusions during the welding process, resulting in poor bonding of the entire fusion surface and a sharp decline in joint performance (see Fig. 3).

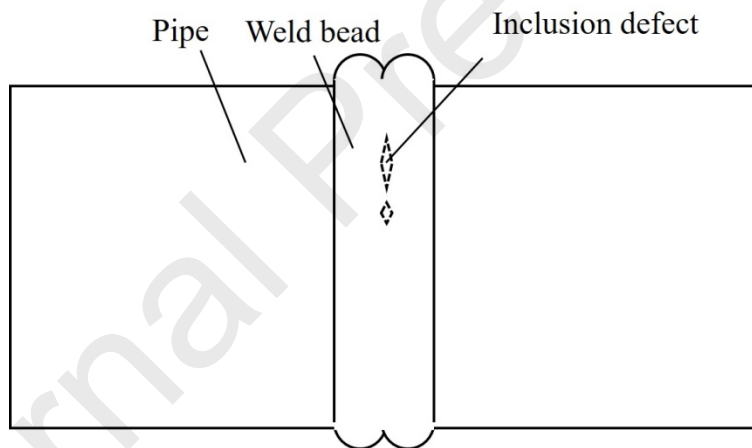


Fig. 3 Schematic of an inclusion defect.

Inclusion defects lead to a worsening of the mechanical properties and the overall failure of the fusion surface, which is manifested as a brittle fracture of the whole fusion surface or an uneven ductile fracture within a large area.

The main causes are:

- 1) The end face of the pipe is not milled, and there is an oxide layer, resulting in a weak or even absent entanglement of the polyethylene molecules on the fusion surface.
- 2) The harsh welding environment and large quantity of dust lead to the formation of inclusions within the fusion surface in the welding process.
- 3) Water, oil, grass leaves, plastic bag fragments, and heterogeneous debris are mixed into the fusion

surface during welding, resulting in a weak or even absent entanglement of the polyethylene molecules after welding.

3. Materials and sample preparation

The commonly used colors for town gas polyethylene pipes are yellow, orange, and black; a black polyethylene pipe material is obtained through mixture with carbon black. In this work, a yellow polyethylene pipe was selected to study the three most common welding defects: incomplete fusion defects, hole defects, and inclusion defects.

A defect test block production method was independently developed for the hot melt welding joints of polyethylene pipes. According to the defect properties of hot melt welding joints, the prefabrication of incomplete fusion defects, hole defects, and inclusion defects was realized by designing the end face structure of the butt pipe. The minimum characteristic size of the prefabricated defects was 1 mm. In the defect prefabrication, the regular defect shape was used as the standard defect shape for assessing the technology as well as for scientific research. Varying the defect shape enables the manufactured defect to be closer to the actual shape of the site, making it more convenient for both simulation and comparison with the actual defects. On the other hand, the fabricated sample had the same curvature characteristics and geometric parameters of real polyethylene pipes to lay a foundation for the non-destructive defect testing of real pipes.

The types and sizes of the produced defect are listed in Table 1, and the defect samples are shown in Fig. 4.

Table 1 Defect types and sizes within a polyethylene-pipe hot melt joint.

Defect type	Defect size (mm)	Defect quantity
Incomplete fusion	Diameters 1, 2, 3, 5	12
Hole	Diameters 1, 2, 3, 5	12
Inclusion	Diameters 1, 2, 3, 5	12

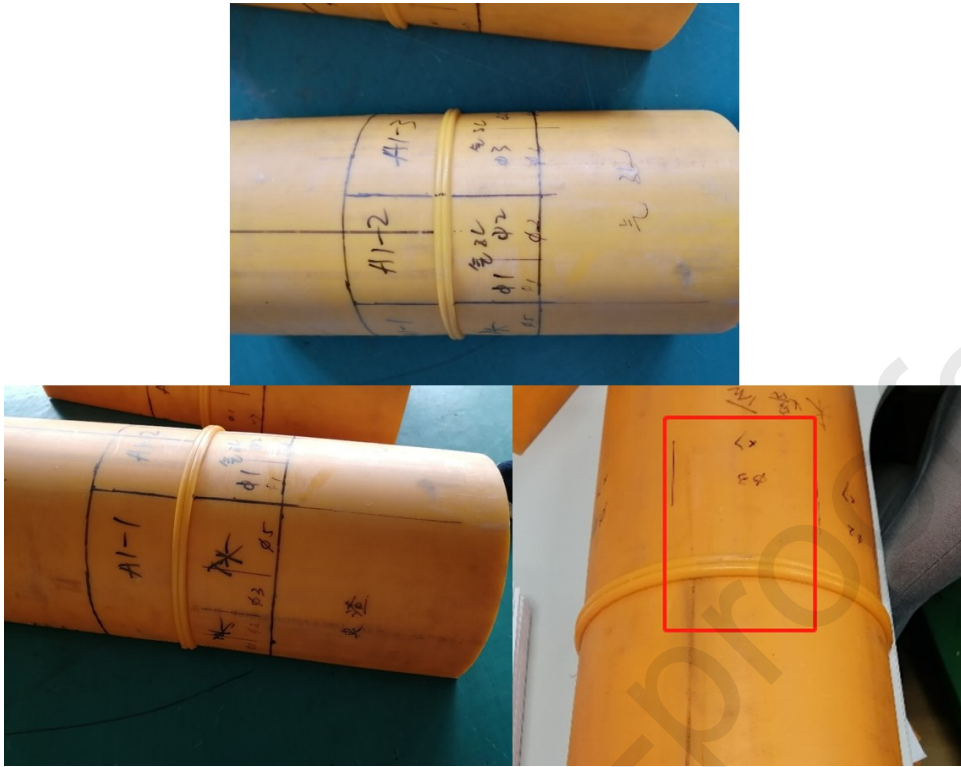
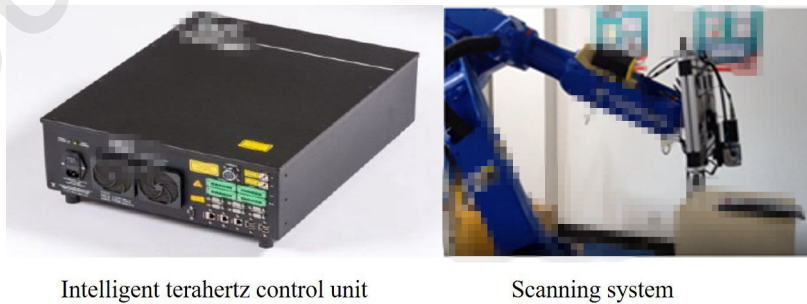


Fig. 4 Defect samples of the hot melt joint as part of the polyethylene pipe.

4. Experimental

4.1 Equipment

An ANTHz-8 THz time-domain spectral system in the reflection detection mode was employed for defect detection testing. The system consists of a data acquisition unit and a data processing unit. The data acquisition unit is a THz reflection probe driven by a mechanical arm. During the detection process, the sample surface is scanned vertically in equidistant mode, and the detection step is 1 mm. The detection data is stored in a computer and then processed using a special software to obtain the defect image. The THz detection equipment is shown in Fig. 5.



Intelligent terahertz control unit

Scanning system

Fig. 5 THz detection equipment.

4.2 Principle of defect detection

The results obtained by a THz time-domain spectral imaging system are actually a set of three-dimensional (3D) space–time (two-dimensional space (x,y) and one-dimensional time) data. These 3D data can be used to further reproduce the THz images of the samples in different-thickness layers. In addition, since the THz image at a time point contains very little information, it is usually necessary to acquire the entire 3D data. The reconstruction of a THz image is usually based on the delay time of specific parameters or the peak of a THz time-domain waveform.

The internal defect detection within the structure can be implemented by observing the B-scan diagram in the detection imaging results. B-scan imaging is performed along the pixel rows and columns in the detection area, where the horizontal axis is the position of the row or column, and the vertical axis is the signal intensity of the corresponding time-of-flight point. The B-scan image can be used to localize and analyze the defect, and the corresponding flight time provides information about the depth direction of the defect. In addition, defect features in the THz time-domain waveform can be extracted to further analyze the tested object.

5. Experimental results and discussion

In order to facilitate path determination during scanning with a robot arm, the hot-melt-joint defect sample was cut into shingles according to the defect type. In the presence of flanged edges, reflective C-scan detection was carried out on the unfused defect specimen. Meanwhile, owing to the excessive curvature of the flanged edge, the robot arm could not achieve a vertical incidence on the flanged surface, so the curvature at the flanged edge was ignored during scanning.

The scanning results obtained for the incomplete fusion defect sample are shown in Fig. 6. In the presence of a flanged edge, the THz wave was detected in the direction perpendicular to the workpiece surface, while the waveform could not be vertically incident on the flanged edge, hindering the detection of the reflected signal. Therefore, the THz detection technology cannot detect the internal defects of hot melt joints with flanged edges.

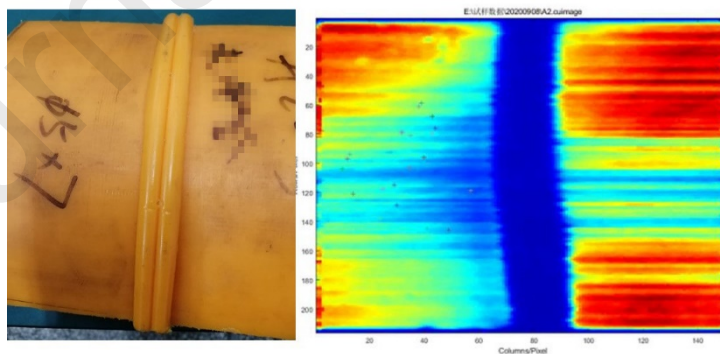


Fig. 6 THz scanning imaging data acquired for a hot-melt-joint sample with a flanged edge and an incomplete fusion defect.

The influence of the flanged edge on the THz detection was analyzed, as shown in Figure 7. In the figure, α stands for the reflection detection mode of the equipment. In this method, the THz wave cannot be vertically incident on the flanged edge surface because of the excessive curvature of the latter; as a result, the reflected wave deviates from the expected path and cannot be sensed by the detector, making

the detected data invalid.

β denotes an improved detection method. Through an appropriate modification of the scanning tool, the scanning path becomes more accurate, and the THz wave is thus perpendicular to the flanged edge surface, which can ensure that the probe can detect the reflected wave. However, the defect information collected in this method is distorted, making the existing tool and probe size still not ideal.

A mode defined as γ corresponds to the tube-body detection method, in which the surface curvature of the tube body is small, whereas the existing scanning tools and probe size can ensure that the incident wave is perpendicular to the surface of the workpiece, allowing the probe to detect the reflected wave and thereby ensuring the reliability and efficiency of the detection.

Through the above analysis, it can be seen that the reflection detection method is not suitable for detecting defects in hot melt joints with flanged edges. On the other hand, the transmission detection method can detect the defects in the flanged edge due to the fact that the detector is placed on the other side of the workpiece and is thus able to detect the transmitted signal. However, the transmission detection method is not suitable for defect detection within field pipelines.

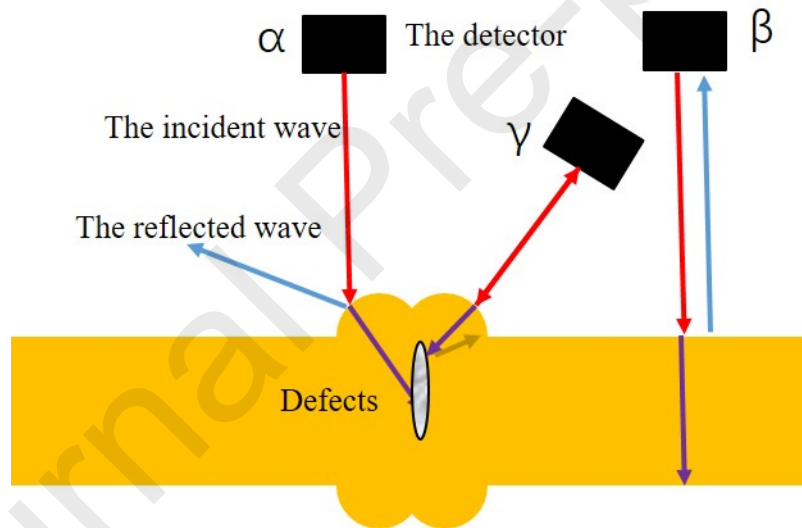
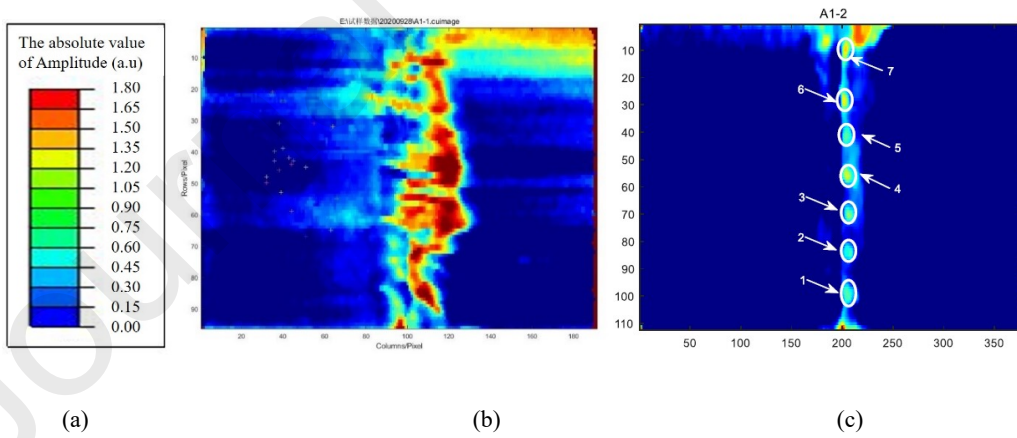


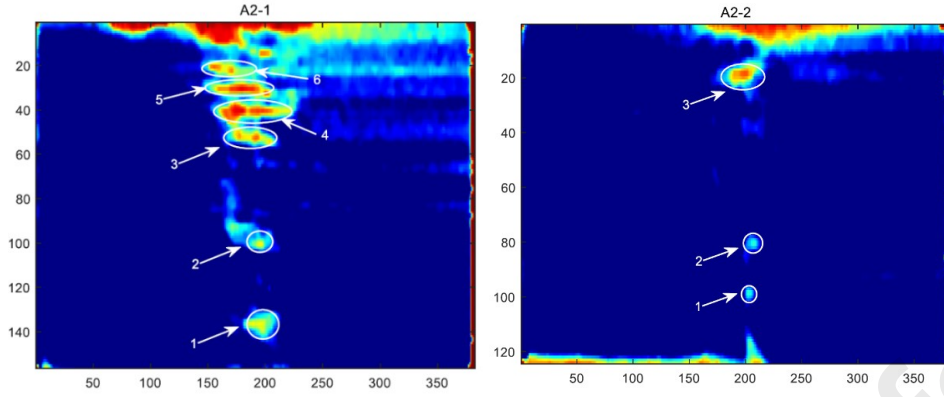
Fig. 7 Analysis of the influence of the flanging of hot melt joints on the THz detection of defects.

In order to eliminate its effect, the flanged edge was polished until it was as flat as the outer surface of the base material, as shown in Fig. 8. THz detection testing was carried out on the sample after removing the flanged edge, and the results are shown in Fig. 9, revealing the identified defects. The different colors in the figure represent the distribution range of defects by converting the reflected amplitude of different positions into different colors. The minimum diameter of the defects detected in the sample was 1 mm, meaning that the THz detection technology can localize incomplete fusion, hole, and inclusion defects with a feature size of at least 1 mm. In summary, when performing reflective THz non-destructive testing of hot melt joints, it is necessary to remove the flanged edge so as to be able to obtain the defect information.



Fig. 8 Photographs of the defect samples and the numbers of hot melt joints after cutting the flanged edges: (a) inclusion defect; (b) hole defect; (c) incomplete fusion defect.





(d)

Fig. 9 THz detection images of unfused defects in hot melt joints after cutting the flanges: (a) color legend; (b) inclusion defect; (c) hole defect; (d) incomplete fusion defect.

The hole defects of a hot-melt-joint specimen were destructively assessed. There were eight prefabricated hole defects; seven actual defects were found through destructive detection, and seven defects were detected using the THz technology, with a defect detection rate of 100%. The size of the detected hole defects was calculated according to the method provided in Ref. [36].

According to the two-dimensional imaging results of the defect, the axial size L_a and circumferential dimension L_w of the defect can be calculated as follows.

Suppose that the axial step detected is X mm and the circumferential dimension detected is Y mm, so the pixel size is $X \text{ mm} \times Y \text{ mm}$.

By measuring the number of axial pixels m of the defect in the two-dimensional image, the axial dimension of the defect can be calculated as:

$$L_a = m \times X. \quad (1)$$

By measuring the number of circumferential pixels n of the defect in the two-dimensional image, the circumferential dimension of the defect can be calculated as:

$$L_w = n \times Y. \quad (2)$$

The calculation results of the defect diameter are shown in Table 2. By comparing the results of destructive detection and THz detection, it can be seen that their discrepancy is less than 15%.

Table 2 Destructive assessment of the defect sizes.

NO.	Prefabricated diameter (mm)	Actual diameter (mm)	Detected diameter (mm)	Detection error (%)

1	5	5.46	5.86	7.32
2	5	5.32	5.92	11.28
3	5	5.42	5.74	5.90
4	3	3.12	3.92	9.62
5	3	3.32	3.88	7.83
6	3	3.36	3.82	13.69
7	2	2.22	2.96	14.41
8	2	2.25	2.92	12

6. Defect signal recognition model

In this section, based on the scanning results obtained on yellow polyethylene pipe hot-melt welding defect samples, the signal recognition models of incomplete fusion, hole, and inclusion defects are developed by analyzing A-scan and C-scan signals, which lay a foundation for the defect signal recognition technology of polyethylene pipes based on THz non-destructive testing.

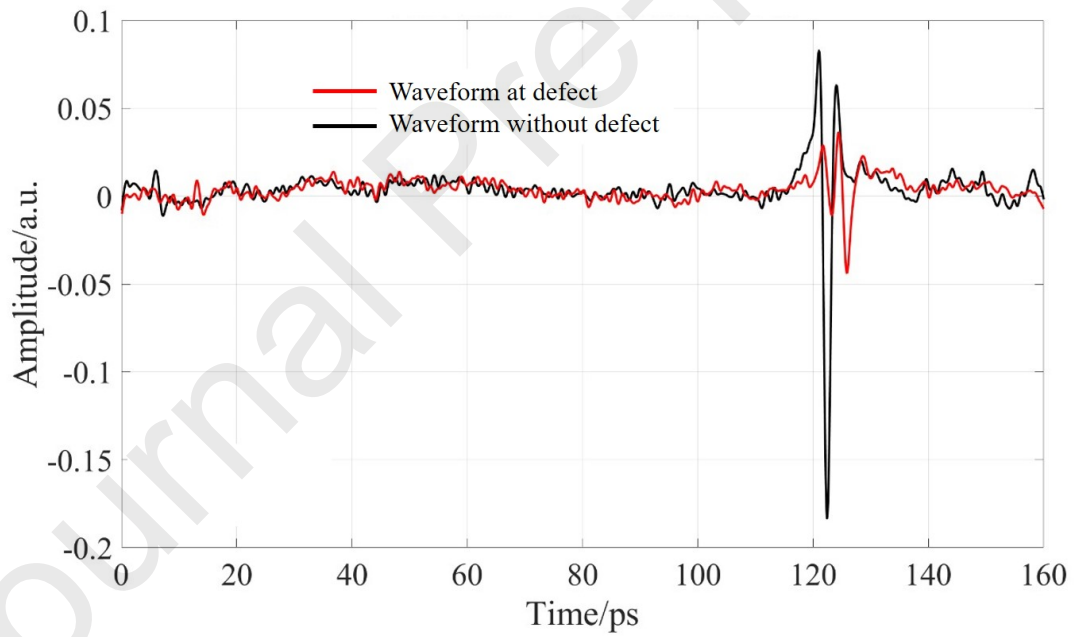
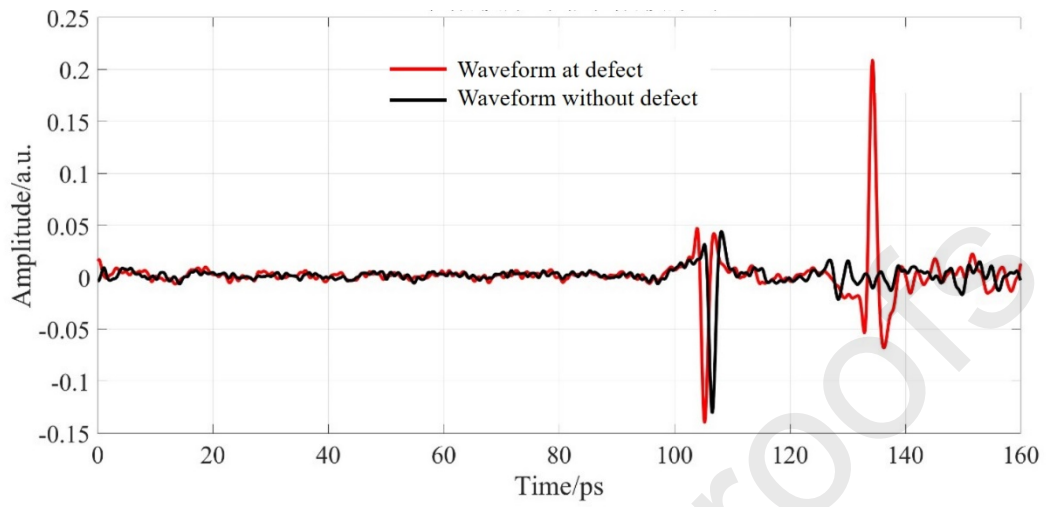
6.1 A-scan signal recognition model

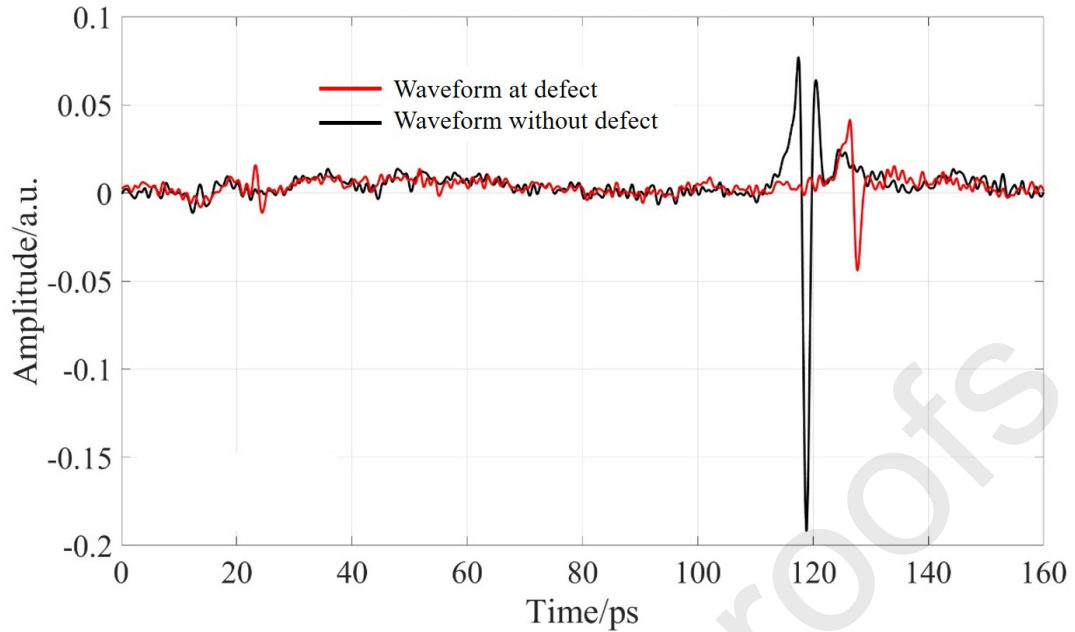
By extracting the single waveform at a defect, the relevant A-scan signal can be obtained. In the defect scanning data on the hot melt joint of the yellow polyethylene pipe, the single waveforms of inclusion, incomplete fusion, and hole defects were extracted, as shown in Fig. 10. According to the figure, the amplitude of the reflected wave in the non-defect area was large, changing from positive to negative and then back to positive in an M-shaped manner, while the reflected signal in the defect area exhibited noticeable variations.

As can be seen from Fig. 10(a), inclusion defects generate two discrete reflected signals, among which the first one is almost the same as the conventional M-shaped signal and is inferior to the second one, whose positive and negative values are opposite to the first signal.

In Fig. 10(b), the reflected signal of hole defects presents multiple continuous peaks, which resemble jagged canine teeth with alternating positive and negative values.

Fig. 10(c) displays the reflected signal of the incomplete fusion defect, which is composed of two continuously changing peaks, one positive and one negative, forming an N-shape.





(c)

Fig. 10 Single waveforms at the defect of a polyethylene-pipe hot melt joint and normal waveforms: (a) inclusion defect; (b) hole defect; (c) incomplete fusion defect.

6.2 C-scan signal recognition model

Through the tomography method, defects can be projected onto the scanning surface, as shown in Fig. 11. In the figure, the longitudinal coordinate corresponds to the expanded projection of the sample circumferential scanning surface, and the horizontal coordinate refers to the expanded projection of the sample axial scanning surface. Therefore, THz C-scanning imaging actually expands the two-dimensional surface into a plane for imaging analysis. The colors in the figure represent the amplitude of the reflected wave at a certain position.

As can be seen from Fig. 11(a), the peculiarities of inclusion defects are as follows: the signal structure of a defect is irregular, exhibiting multiple bar branches and sharp contours. According to Fig. 11(b), the imaging characteristics of hole defects consist of features distributed along the girth of the weld in a long strip, revealing a smooth outline without any edges as well as of features distributed along the middle line of the weld, with little differences between axial and circumferential dimensions. As can be seen from Fig. 11(c), the features of the incomplete fusion defects are as follows: a smooth outline without any edges is distributed along the middle line of the weld in an irregular manner, and the defects appear as long strips along the axis.

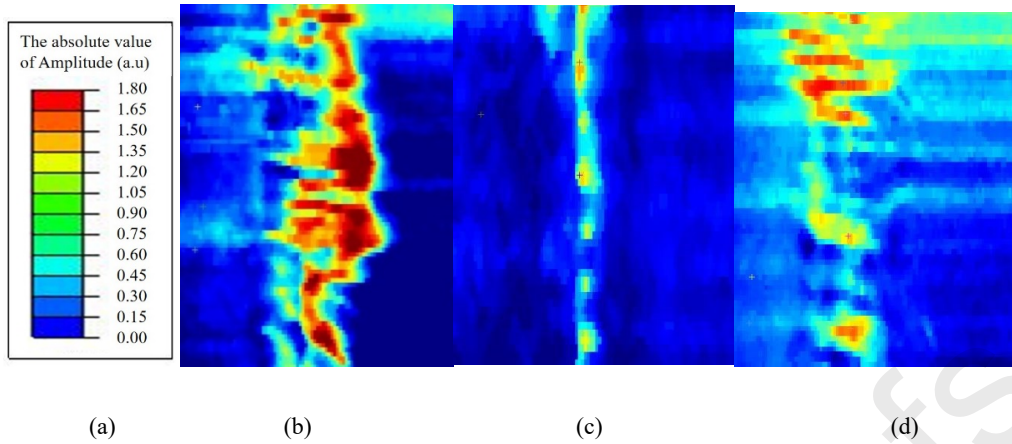


Fig. 11 Defect characteristics of polyethylene-pipe hot melt joints: (a) color legend; (b) inclusion defects; (c) hole defects; (d) incomplete fusion defects.

6.3 Summary of THz signal analysis techniques for defect detection in polyethylene-pipe hot melt joints

Compared with other NDT technologies, THz detection permits the localization as well as the qualitative and quantitative analysis of non-metallic pipe defects through 3D imaging. The main results obtained in this work regarding the THz detection technology for identifying defects in polyethylene pipes are summarized in Table 2.

Table 2 Technical table for the THz detection analysis of polyethylene-pipe defects.

Defect type	Defect scan mode	
	A-scan	C-scan
Incomplete fusion	The reflected signal of the incomplete fusion defect presents two continuously changing peaks, one positive and one negative, forming an N-shape.	A smooth outline without edges is distributed along the middle line of the weld in an irregular manner, and the defects appear as long strips along the axis.
Hole	The reflected signal of hole defects presents multiple continuous peaks with alternating positive and negative amplitudes resembling jagged canine teeth.	The defects are distributed along the girth of the weld in a long strip, revealing a smooth outline without edges, but also along the middle line of the weld, exhibiting little differences in axial and circumferential dimensions.

Inclusion	Inclusion defects generate two discrete reflected signals, among which the first one is almost the same as the normal (M-shaped) signal and is inferior to the second one, whose positive and negative values are opposite to the first signal, forming an inverted M-shape.	The signal structure of the defect image is irregular, possessing multiple bar branches and sharp contours.
------------------	--	---

7. Conclusion

The typical defect test blocks of a polyethylene-pipe hot melt joint were prepared, namely incomplete fusion, hole, and inclusion defects, whose characteristic size was at least 1 mm. Using the THz time-domain scanning imaging technology, non-destructive testing was carried out on defect samples of the hot melt joint of a yellow polyethylene pipe, and the following conclusions were drawn.

(1) The THz technology cannot detect the internal defects within the hot melt joint because of the existence of the flanged edge. After removing the flanged edge, defects such as incomplete fusion, hole, and inclusion defects inside the hot melt joint can be detected. This indicates that flanged edges must be removed when using the THz technology for detecting defects in hot melt joints.

(2) The minimum detectable diameter of the prefabricated hot melt joint defects is 1 mm. However, due to the limitations of the defect manufacturing process, the possibility of detecting a smaller defect size has not been evaluated.

(3) The relationship between the defect type of the polyethylene pipe and the THz wave detection signal was established. For the A-scan mode, the defect type can be identified according to the number and shape of the reflected wave crest, while for the C-scan mode, the defect type can be identified according to the structural features of the two-dimensional image of the detected signal.

8. Acknowledgments

This work was supported by the Natural Science Foundation of Shaanxi Province (grant no. 2021JQ-947), the Basic Research and Strategic Reserve Technology Research Fund of the China National Petroleum Corporation (projects nos. 2019D-5008 (2019Z-01) and 2022DQ03 (2022Z-03)), and the Youth Science and Technology New Star Project of Shaanxi Province (grants nos. 2021KJXX65 and 2023KJXX-092).

9 References

- [1] An Investigation of Non-Metallic Pipe for Use With Liquid Corrosives. *Corrosion* 1960; 16: 25–30. doi:10.5006/0010-9312-16.2.25
- [2] Zubail A, Traidia A, Masulli M, et al. Carbon and energy footprint of nonmetallic composite pipes

- in onshore oil and gas flowlines. *J Clean Prod* 2021; 305: 127150. doi:10.1016/j.jclepro.2021.127150
- [3] Bai B. A millimeter-wave technique for nondestructive testing on nonmetallic materials. In: *International Conference on Millimeter Wave & Far Infrared Science & Technology*. 1996
- [4] Green WH, Wells JM. Characterization of impact damage in metallic/nonmetallic composites using x-ray computed tomography imaging. In: *American Institute of Physics Conference Series*. 1999: 622–629
- [5] Amineh RK, Ravan M, Sharma R. Non-Destructive Testing of Non-Metallic Pipes Using Wideband Microwave Measurements. *IEEE Trans Microw Theory Tech* 2020; PP. doi:10.1109/TMTT.2020.2969382
- [6] Kalinichenko NP, Kalinichenko AN, Konareva IS. Reference specimens of nonmetallic materials for penetrant nondestructive testing. 2011; 47: 663–666. doi:10.1134/s1061830911100081
- [7] Feng JH. *Research on Nonlinear Ultrasonic Modulation Detection Technology for Nonmetallic Pipeline Structure Damage*. South China University of Technology; 2016
- [8] Hai LG, Shen GT, Nian LH. *Nondestructive Testing of Pressure Vessels: Nondestructive Testing Technique for Nonmetallic Pressure Vessels*. *Nondestruct Test* 2005;
- [9] Zhong-Qiang JU, Zhang MJ, Zhang JW, et al. *Nondestructive Testing of Cast in Pipe Castings*. *J Netshape Form Eng* 2018;
- [10] Schneider H. The nondestructive testing of tubes and pipes for nuclear application. *Nucl Eng Des* 1984; 81: 69–76. doi:10.1016/0029-5493(84)90252-8
- [11] Ng CT, Veidt M, Lam HF, et al. APPLICATION OF BAYESIAN APPROACH FOR DAMAGE CHARACTERIZATION IN BEAMS UTILIZING GUIDED WAVES. San Diego, California, (USA); 2011: 705–712
- [12] Cheraghi N, Riley MJ, Taheri F. A novel approach for detection of damage in adhesively bonded joints in plastic pipes based on vibration method using piezoelectric sensors. 2005
- [13] Bareille O, Kharrat M, Zhou W, et al. Distributed piezoelectric guided-T-wave generator, design and analysis. *Mechatronics* 2012; 22: 544–551. doi:10.1016/j.mechatronics.2011.11.005
- [14] Pau A, Vestroni F. Damage characterization in a bar using guided waves. : 10
- [15] Redo-Sanchez, A., Xi-Cheng, et al. Terahertz Science and Technology Trends. *Sel Top Quantum Electron IEEE J Of* 2008; 14: 260–269. doi:10.1109/JSTQE.2007.913959
- [16] TAOGLAS. White 2.4 / 5.8 GHz Dual Band 3-3.5dBi Rubber Duck Dipole Antenna with RP-SMA(M). Accessed: Mar. 1, 2022. [Online]. Available: <https://cdn3.taoglas.com/datasheets/GW.48.A151W.pdf>
- [17] Makhoulouf D, Choubani M, Saidi F, et al. Enhancement of transition lifetime, linear and nonlinear

optical properties in laterally coupled lens-shaped quantum dots for Tera-Hertz range. *Phys E Low-Dimens Syst Nanostructures* 2018; 103: 87–92. doi:10.1016/j.physe.2018.05.024

[18] Pani S, Tripathy MR, Kumar A. Analysis of rectangular patch array antenna on circular plane for Tera Hertz applications. *Optik* 2019; 188: 302–307. doi:10.1016/j.ijleo.2019.05.034

[19] Shah SIH, Lim S. Review on recent origami inspired antennas from microwave to terahertz regime. *Mater Des* 2021; 198: 109345. doi:10.1016/j.matdes.2020.109345

[20] Christy SPJ, Suganthi J, Kavitha S, et al. Ring monopole antenna for Tera-Hertz application. *Mater Today Proc* 2021; 45: 1827–1833. doi:10.1016/j.matpr.2020.09.003

[21] Wahaia F, Valusis G, Bernardo LM, et al. Detection of colon cancer by terahertz techniques. *J Mol Struct* 2011; 1006: 77–82. doi:10.1016/j.molstruc.2011.05.049

[22] Yang K, Abbasi QH, Chopra N, et al. Effects of non-flat interfaces in human skin tissues on the in-vivo Tera-Hertz communication channel. *Nano Commun Netw* 2016; 8: 16–24. doi:10.1016/j.nancom.2015.09.001

[23] Yao-Chun, Shen. Terahertz pulsed spectroscopy and imaging for pharmaceutical applications: A review. *Int J Pharm* 2011; 417: 48–60. doi:10.1016/j.ijpharm.2011.01.012

[24] Scheller M, Jansen C, Koch M. Analyzing sub-100- μm samples with transmission terahertz time domain spectroscopy. *Opt Commun* 2009; 282: 1304–1306. doi:10.1016/j.optcom.2008.12.061

[25] Wang Q, Ma YH. Qualitative and quantitative identification of nitrofen in terahertz region. *Chemom Intell Lab Syst* 2013; 127: 43–48. doi:10.1016/j.chemolab.2013.05.011

[26] Taday PF, Bradley IV, Arnone DD. Terahertz pulse spectroscopy of biological materials: L-glutamic Acid. *J Biol Phys* 2003; 29: 109. doi:10.1023/A:1024424205309

[27] Yu B, Zeng F, Yang Y, et al. Torsional Vibrational Modes of Tryptophan Studied by Terahertz Time-Domain Spectroscopy. *Biophys J* 2004; 86: 1649–1654. doi:10.1016/S0006-3495(04)74233-2

[28] Federici JF, Schulkin B, Huang F, et al. THz imaging and sensing for security applications—explosives, weapons and drugs. *Semicond Sci Technol* 2005; 20: S266–S280. doi:10.1088/0268-1242/20/7/018

[29] Wang J, Zhang J, Chang T, et al. Terahertz nondestructive imaging for foreign object detection in glass fibre-reinforced polymer composite panels. *Infrared Phys Technol* 2019; doi:10.1016/j.infrared.2019.02.003

[30] Allis DG, Zeitler JA, Taday PF, et al. Theoretical analysis of the solid-state terahertz spectrum of the high explosive RDX. *Chem Phys Lett* 2008; 463: 84–89. doi:10.1016/j.cplett.2008.08.014

[31] ZHANG Dan-dan, REN Jiao-jiao, LI Lijuan, et al. Terahertz Non-destructive Testing Technology for Glass Fiber Honeycomb Composites. *Acta Photonica Sinica*, 2019, 48(2):0212002

- [32] Ospald F, Zouaghi W, Beigang R, et al. Aeronautics composite material inspection with a terahertz time-domain spectroscopy system. *Opt Eng* 2013; 53: 123–128. doi:10.1117/1.oe.53.3.031208
- [33] B CJA, B SWA, C HW, et al. Terahertz spectroscopy on adhesive bonds. *Polym Test* 2011; 30: 150–154. doi:10.1016/j.polymertesting.2010.11.005
- [34] Ariyoshi S, Hashimoto S, Ohnishi S, et al. Broadband terahertz spectroscopy of cellulose nanofiber-reinforced polypropylenes. *Mater Sci Eng B* 2021; 265: 115000. doi:10.1016/j.mseb.2020.115000
- [35] Thomas DH, Cordes AH, Weid J. Nondestructive evaluation of glued joints in nonmetallic samples using THz waves. In: *International Conference on Infrared*. 2012
- [36] Hailiang Nie, Fengdan Hao, Litao Wang, et al. Application of Terahertz Nondestructive Testing Technology in the Detection of Polyethylene Pipe Defects. *ACS Omega* 2023 8 (30), 27323-27332. DOI: 10.1021/acsomega.3c02701

Highlights:

1. A novel and reliable method for nondestructive testing of typical defects in PE pipes based on terahertz detection technology.
2. An effective detection scheme that can distinguish the minimum 2 mm feature size of prefabricated defects experimentally.
3. The first establishment of the corresponding rule between the characteristic defects of PE pipe and the detection signals of THZ wave.

Declaration of interests

The authors declare that they have no known competing financial interests or personal relationships that could have appeared to influence the work reported in this paper.

The authors declare the following financial interests/personal relationships which may be considered as potential competing interests: